

UC Berkeley

UC Berkeley Previously Published Works

Title

Cross sections and calculated yields of some radionuclides of yttrium, strontium and rubidium formed in proton-induced reactions on enriched strontium-86: possibility of production of ^{85}gSr , ^{83}Rb and $^{82\text{m}}\text{Rb}$ in no-carrier-added form

Permalink

<https://escholarship.org/uc/item/6tx4x57r>

Journal

Radiochimica Acta, 111(2)

ISSN

0033-8230

Authors

Uddin, M Shuza
Basunia, M Shamsuzzoha
Spahn, Ingo
[et al.](#)

Publication Date

2023-02-01

DOI

10.1515/ract-2022-0086

Peer reviewed

M. Shuza Uddin*, M. Shamsuzzoha Basunia, Ingo Spahn, Stefan Spellerberg, Rahat Khan, M. Mezbah Uddin, Lee A. Bernstein, Bernd Neumaier and Syed M. Qaim

Cross sections and calculated yields of some radionuclides of yttrium, strontium and rubidium formed in proton-induced reactions on enriched strontium-86: possibility of production of ^{85g}Sr , ^{83}Rb and ^{82m}Rb in no-carrier-added form

<https://doi.org/10.1515/ract-2022-0086>

Received August 31, 2022; accepted November 9, 2022;

published online November 29, 2022

Abstract: Cross sections of the $^{86}\text{Sr}(p,3n)^{84m}\text{Y}$, $^{86}\text{Sr}(p,\alpha)^{82m}\text{Rb}$, and $^{86}\text{Sr}(p,x)^{85g}\text{Sr}$ reactions were measured from their respective thresholds up to 16.2 MeV and from 23.0 to 44.1 MeV at FZJ, and from 14.3 to 24.5 MeV at LBNL, using 96.4% enriched $^{86}\text{SrCO}_3$ as target material. Thin targets prepared by sedimentation were irradiated with protons in a stacked-form, and the induced radioactivity was measured by high-resolution γ -ray spectrometry. Nuclear model calculations based on the code TALYS reproduced our experimental cross section data well. From the excitation functions, the integral yields of the above three radionuclides were calculated. The yield of ^{85g}Sr via the $^{nat}\text{Sr}(n,\gamma)$ process was also measured using the TRIGA Mark-II reactor at AERE, Savar. A comparison of the reactor and cyclotron production of carrier-added ^{85g}Sr is given. The production possibilities of the three investigated radionuclides

in no-carrier-added forms at a 30 MeV cyclotron via new routes are discussed.

Keywords: $^{86}\text{SrCO}_3$ thin samples; cyclotrons and TRIGA Mark II reactor; excitation function; integral yield and isotopic purity of the product; nuclear model calculation; proton- and neutron-irradiations.

1 Introduction

The first three adjacent elements of the 5th Period of the Periodic Table of Elements, namely rubidium, strontium and yttrium, occurring in well-defined chemical valence states of 1^+ , 2^+ , and 3^+ , respectively, have several radioisotopes suitable for applications in medicine and other tracer studies [cf. 1, 2]. In the case of monovalent rubidium, for example, the short-lived ^{82}Rb ($T_{1/2} = 1.3$ min), available via the ^{82}Sr ($T_{1/2} = 25.3$ day)/ ^{82}Rb generator system, finds wide application in myocardial perfusion investigations using positron emission tomography (PET). In addition, the radionuclide ^{82m}Rb ($T_{1/2} = 6.3$ h) has been suggested as a potential longer lived substitute for the short-lived ^{82}Rb . Furthermore, the radionuclide ^{81}Rb ($T_{1/2} = 4.58$ h) is used in the form of the $^{81}\text{Rb}/^{81m}\text{Kr}$ ($T_{1/2} = 13.3$ s) generator for lung ventilation studies, employing the short-lived krypton gas, and imaging via single photon emission computed tomography (SPECT). As regards the divalent strontium, the β^- -emitting radionuclide ^{89}Sr ($T_{1/2} = 50.5$ day) has been found to be very effective in reducing the pain due to prostate and bone cancer. In addition, the radionuclides ^{83}Sr ($T_{1/2} = 32.4$ h) and ^{85g}Sr ($T_{1/2} = 64.9$ day) are also useful, the former as a positron-emitting partner of the “matched” theranostic pair $^{83}\text{Sr}/^{89}\text{Sr}$ [cf. 3] and the latter as a useful tracer in agricultural and environmental studies. In fact ^{85g}Sr is the only longer lived tracer of strontium which can be conveniently used. Furthermore, the radionuclide ^{87m}Sr ($T_{1/2} = 2.8$ h), obtained via the ^{87}Y ($T_{1/2} = 80.3$ h)/ ^{87m}Sr

*Corresponding author: M. Shuza Uddin, Institut für Neurowissenschaften und Medizin, INM-5: Nuklearchemie, Forschungszentrum Jülich, D-52425 Jülich, Germany; and Institute of Nuclear Science and Technology, Atomic Energy Research Establishment, Savar, Dhaka, Bangladesh, E-mail: md.shuzauddin@yahoo.com

M. Shamsuzzoha Basunia, Nuclear Science Division, Lawrence Berkeley National Laboratory, Berkeley, CA 94720, USA

Ingo Spahn, Stefan Spellerberg, Bernd Neumaier and Syed M. Qaim, Institut für Neurowissenschaften und Medizin, INM-5: Nuklearchemie, Forschungszentrum Jülich, D-52425 Jülich, Germany

Rahat Khan, Institute of Nuclear Science and Technology, Atomic Energy Research Establishment, Savar, Dhaka, Bangladesh

M. Mezbah Uddin, Centre for Research Reactor, Atomic Energy Research Establishment, Savar, Dhaka, Bangladesh

Lee A. Bernstein, Nuclear Science Division, Lawrence Berkeley National Laboratory, Berkeley, CA 94720, USA; and Department of Nuclear Engineering, UC Berkeley, Berkeley, CA 94720, USA

generator system, finds application in bone scanning, utilizing SPECT imaging. As far as the trivalent element yttrium is concerned, the radionuclide ^{90}Y ($T_{1/2} = 2.7$ day), obtained generally via the ^{90}Sr ($T_{1/2} = 28.5$ a)/ ^{90}Y generator, is commonly used in radionuclide targeted therapy and its β^+ -emitting partner ^{86g}Y ($T_{1/2} = 14.7$ h) serves to determine the dose distribution accurately via PET scanning [cf. 3, 4]. Thus, further investigations on the production methodologies of the above-mentioned radioisotopes as well as of some other potentially useful radioisotopes of those three elements appear to be of considerable value.

In two recent studies on the interactions of protons with ^{86}Sr , accurate cross sections were measured for the production of the medically important radionuclide ^{86g}Y [5] as well for the formation of the isomeric states $^{86m,g}\text{Y}$ and $^{85m,g}\text{Y}$ from the theoretical point of view [6]. Some additional data on the formation of a few other radionuclides were also obtained which are being reported in this paper. Furthermore, thick target yields of all investigated products have been calculated. Therefrom, the production possibilities of the useful or potentially useful radionuclides ^{85g}Sr , ^{83}Rb , and ^{82m}Rb in no-carrier-added form via new routes are deduced. The decay data of the radionuclides being treated in some detail in this work are summarized in Table 1 (taken from [7]).

Regarding the known production methodologies of the above-mentioned three radionuclides, ^{85g}Sr is generally obtained in small amounts via the $^{84}\text{Sr}(n,\gamma)$ -reaction in a nuclear reactor using a $^{\text{nat}}\text{Sr}$ target. However, the

abundance of ^{84}Sr in $^{\text{nat}}\text{Sr}$ is only 0.56% and σ_{th} for the process is also small. The resulting yield and specific activity of ^{85g}Sr are therefore low. The radionuclide is commercially available with low specific activity for tracer studies but also as a standard for γ -ray spectroscopy (e.g. from Eckert and Ziegler, Berlin). From the cross sections measured for the $^{85}\text{Rb}(p,n)^{85g}\text{Sr}$ [8] and $^{\text{nat}}\text{Rb}(p,xn)^{85g}\text{Sr}$ [9, 10] reactions it is deduced that higher specific activity product could be obtained. We discuss here a new production route, namely $^{85m,g}\text{Y} \rightarrow ^{85g}\text{Sr}$ precursor system. Regarding the radionuclides ^{83}Rb and ^{82m}Rb , production yields can be calculated from the known excitation functions of the reactions $^{83}\text{Kr}(p,n)^{83}\text{Rb}$ [11] and $^{82}\text{Kr}(p,n)^{82m}\text{Rb}$ [12]. In the present work, we discuss new possible production routes of those two radionuclides as well.

2 Experimental

2.1 Samples and irradiations at cyclotrons

Details on sample preparation technique, irradiations at several cyclotrons and radioactivity measurement of several radionuclides produced in the interactions of protons with ^{86}Sr have been reported in two recent publications [5, 6]. Therefore, in this paper we give only a very short description of some salient aspects of production of a few potentially useful radionuclides. Thin samples of enriched $^{86}\text{SrCO}_3$ (isotopic composition: 96.4% ^{86}Sr ; 1.33% ^{87}Sr ; 2.26% ^{88}Sr , supplied by Eurisotop, France) were prepared by the sedimentation technique

Table 1: Decay data of the investigated radionuclides* (taken from NUDAT [7]).

Radionuclide	Production reaction	Q-value (MeV)	Decay mode (%)	Half-life	γ -ray energy (keV)	γ -ray intensity (%)
^{84m}Y	$^{86}\text{Sr}(p,3n)$	-27.622	$\beta^+ = 84$	39.5 (8) min	793.1	98.3 (4)
					974.3	78 (4)
					660.6	11.3 (4)
					1039.7	56 (3)
^{85m}Sr	$^{86}\text{Sr}(p,pn)$	-9.505	$IT = 86.6$	67.63 (4) min	231.86	83.9 (16)
	$^{86}\text{Sr}(p,2n)^{85m}\text{Y} \rightarrow ^{85m}\text{Sr}$	-15.55	$EC = 13.4$			
	$^{86}\text{Sr}(p,2n)^{85g}\text{Y} \rightarrow ^{85m}\text{Sr}$	-15.53				
^{85}Sr	$^{86}\text{Sr}(p,pn)$	-9.27	$EC = 100$	64.849 (7) day	514	96 (4)
	$^{86}\text{Sr}(p,pn)^{85m}\text{Sr} \rightarrow ^{85}\text{Sr}$	-9.51				
	$^{86}\text{Sr}(p,2n)^{85m}\text{Y} \rightarrow ^{85}\text{Sr}$	-15.55				
	$^{86}\text{Sr}(p,2n)^{85g}\text{Y} \rightarrow ^{85}\text{Sr}$	-15.53				
^{83}Rb	$^{86}\text{Sr}(p,\alpha)$	-0.59	$EC = 100$	86.2 (1) day	520.40	44.7 (33)
	$^{86}\text{Sr}(p,2p2n)$	-28.88			529.59	29.3 (21)
	$^{86}\text{Sr}(p,^3\text{He}n)$	-21.17				
^{82m}Rb	$^{86}\text{Sr}(p,\alpha n)$	-11.61	$\beta^+ = 21.2$	6.472 (6) h	554.35	62.4 (9)
			$EC = 78.8$		619.11	37.98 (9)

*Data for other isotopes of Y, Sr, and Rb used in two previous investigations were given in relevant publications [5, 6].

and irradiated in several stacks with low-current proton beams at three cyclotrons, namely 88-Inch cyclotron at the Lawrence Berkeley National Laboratory (LBNL), USA, and the cyclotrons BC1710 and JULIC at the Forschungszentrum Jülich (FZJ), Germany. The beam current was measured by charge collection and via the $^{nat}\text{Cu}(p,x)^{62}\text{Zn}$ and $^{nat}\text{Cu}(p,x)^{65}\text{Zn}$ monitor reactions whose cross sections are known very well [13]. The radioactivity of each product was determined through high-resolution γ -ray spectroscopy.

2.2 Samples and irradiations at TRIGA Mark-II research reactor

For determining the ^{85g}Sr -activity formed via the $^{84}\text{Sr}(n,\gamma)$ reaction, SrCl_2 (99.9% purity; LEICO Industries, New York) having natural isotopic composition of strontium, was used as target material. A 10 mg powder sample of SrCl_2 was weighed, placed in a polyethylene bag, heat sealed and finally sandwiched between a thin Ni foil (29 mg, 1 cm diameter) and a Au foil (8.8 mg, 1 cm diameter). Similarly, another set of 18 mg SrCl_2 sample was prepared. The Au foils were used to determine thermal and epithermal neutron fluxes, whereas the Ni foils were used to monitor the fast neutron flux. The above two sets of samples were placed in a single irradiation vial and irradiated in the core of the 3 MW TRIGA Mark-II reactor installed at the campus of Atomic Energy Research Establishment in Savar. A brief description of the basic characteristics of the reactor has been given [cf. 14]. During irradiation the reactor power was kept constant at 500 kW and the irradiation time was 20 min. After irradiation the samples were taken out of the reactor core but kept in the transfer tube for two days to allow decay of the unwanted short-lived radionuclides as well as to reduce the radiation dose to the permissible level. Thereafter, the radioactivities produced in the irradiated strontium samples and the monitor foils were measured nondestructively using a HPGe γ -ray detector (Canberra, 40% relative efficiency, 1.9 keV resolution at 1332.6 keV γ -ray of ^{60}Co) associated with a digital gamma spectrometry system (ORTEC DSPEC jrTM) and Maestro data acquisition software. All the samples and monitor foils were counted at 5 cm from the detector surface. The counting was repeated three times in weekly intervals.

3 Data analysis

In this work we report the new cross section data for the formation of ^{84m}Y , ^{85g}Sr , and ^{82m}Rb via the proton induced activation of ^{86}Sr . Measurements on the short-lived radionuclides ^{84m}Y and ^{82m}Rb were done at FZJ within a few hours after the end of bombardment (EOB). In the case of ^{85g}Sr , on the other hand, measurements were done both at LBNL and FZJ several days after the EOB, so that the short-lived ^{85m}Y , ^{85g}Y , and ^{85m}Sr had all decayed to ^{85g}Sr . A very special care was needed to perform the analysis of the γ -ray spectrum because the characteristic γ -ray of ^{85g}Sr , has the energy 514 keV which is close to the 511 keV β^+ annihilation peak emitted by other radionuclides. Using the Fitzpeak gamma analysis software [15], however, the net peak area

of the 514 keV line could be conveniently determined. A typical analysis of the γ -ray spectrum in the vicinity of the annihilation radiation has been recently presented [16]. The resulting cross section for ^{85g}Sr was a cumulative value of the decay (of ^{85m}Y , ^{85g}Y , and ^{85m}Sr) and direct formation (via the $^{86}\text{Sr}(p,pn)$ -reaction). The uncertainties of the reported cross sections were estimated as described earlier [5, 6].

A typical γ -ray spectrum of the SrCl_2 target irradiated in the research reactor is shown in Figure 1. This spectrum was taken 18 days after the end of bombardment and the measurement was performed for 25,000 s. The peak at 514 keV emitted in the decay of ^{85g}Sr is clearly visible and separable from the annihilation radiation at 511 keV. Due to complete decay of short-lived radionuclides, the annihilation peak at 511 keV was weak. No peak due to decay of ^{83}Sr was visible in the spectrum. This was due to the expected low integral cross section of the $^{84}\text{Sr}(n,2n)$ reaction [17], the low isotopic abundance of ^{84}Sr (0.56%) in natural strontium and the relatively low fast neutron flux. On this basis we assume that the contribution of the $^{86}\text{Sr}(n,2n)^{85g}\text{Sr}$ reaction to total production of ^{85g}Sr should also be negligible under the present experimental condition.

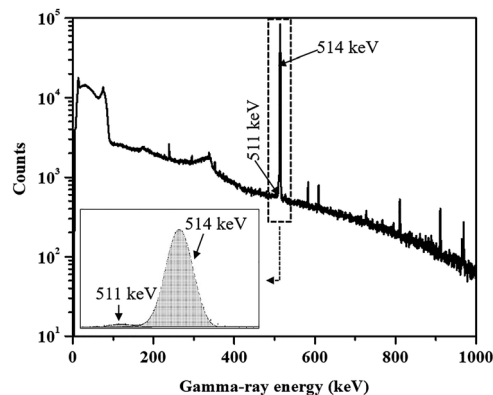


Figure 1: A typical γ -ray spectrum of the $^{nat}\text{SrCl}_2$ sample taken 18 days after irradiation with neutrons in the core of the TRIGA Mark-II research reactor at Savar: an expanded form of the spectrum around the peak at 514 keV is given in the inset.

4 Nuclear model calculations

The cross sections of the reactions $^{86}\text{Sr}(p,\alpha)^{82m}\text{Rb}$, $^{86}\text{Sr}(p,3n)^{84m}\text{Y}$, and $^{86}\text{Sr}(p,x)^{85g}\text{Sr}$ were calculated theoretically by using the TALYS-1.8 code, developed by Koning et al. [18]. This code incorporates several nuclear models to

calculate all the significant nuclear reaction mechanisms over the energy range of 1 keV–200 MeV. In general, the results obtained for proton-induced reactions using global set of parameters, as expressed in the TENDL file [19], give only approximate values. Special care regarding the choice of the input parameters is necessary to reproduce the experimental data [cf. 5, 6]. A few free parameters of the nuclear reaction models are optical model potential, level density formalism, spin distribution of the level density, γ -ray strength function, etc. These values are generally varied within the recommended limits [20]. The spin distribution of the level density is characterized by the ratio of the effective moment of inertia to the rigid-body moment of inertia ($\eta = \Theta_{\text{eff}}/\Theta_{\text{rigid}}$). For the best fitting of our ^{82m}Rb data $\eta = 0.95$ was used, and for ^{84m}Y and ^{85g}Sr the values of $\eta = 0.55$ and $\eta = 0.50$, respectively, were used. Those values were obtained from the systematics based on the evaluation by Sudár and Qaim [21]. The radionuclide ^{85g}Sr is formed via the (p,pn) reaction as well as via the decay of ^{85m}Y , ^{85g}Y , and ^{85m}Sr . Those four

contributions were calculated and summed; the result is compared with the experimentally measured cumulative data.

5 Results and discussion

5.1 Charged-particle induced reactions

5.1.1 Cross sections

The measured cross sections for the three proton induced reaction products, ^{84m}Y , ^{85g}Sr , and ^{82m}Rb , investigated in this work are given in Table 2. The respective uncertainties are also given; they amount to between 8 and 15% (for details cf. [5, 6]). The excitation functions are shown in Figures 2–4. The data for ^{84m}Y (Figure 2) are reported for the first time. The shape of the excitation function is smooth and the data are reproduced by the TALYS calculation fairly well while using an η value of 0.55. With

Table 2: Cross sections of some additional reaction products* formed in protons on ^{86}Sr .

Proton energy (MeV)	Cyclotron	Cross section (mb)		
		$^{86}\text{Sr}(p,3n)^{84m}\text{Y}$	$^{86}\text{Sr}(p,x)^{85}\text{Sr}$	$^{86}\text{Sr}(p,\alpha n)^{82m}\text{Rb}$
44.1 ± 0.3	JULIC	107 ± 12		7.6 ± 1.0
42.7 ± 0.3		116 ± 11	254 ± 24	8.8 ± 1.0
40.3 ± 0.3		136 ± 12	261 ± 24	11.8 ± 1.4
39.1 ± 0.3		138 ± 15		14.9 ± 1.7
37.9 ± 0.3		136 ± 12	301 ± 28	15.5 ± 1.9
36.4 ± 0.3		124 ± 12		
34.9 ± 0.4		103 ± 9	323 ± 28	24.3 ± 3.0
32.6 ± 0.4		83 ± 8		
31.7 ± 0.4		69 ± 7	452 ± 40	33.6 ± 3.3
29.8 ± 0.4		18 ± 2		29.0 ± 2.5
27.6 ± 0.4			673 ± 59	24.8 ± 2.2
26.7 ± 0.4			714 ± 63	21.8 ± 2.0
25.2 ± 0.4			824 ± 72	15.2 ± 1.6
23.0 ± 0.4			871 ± 76	
24.5 ± 0.4	88-inch		872 ± 85	8.5 ± 0.8
22.5 ± 0.4			793 ± 77	2.8 ± 0.3
20.5 ± 0.4			766 ± 75	0.3 ± 0.03
18.4 ± 0.5			546 ± 53	
17.0 ± 0.5			305 ± 30	
15.7 ± 0.5			126 ± 12	
14.3 ± 0.5			6.2 ± 0.6	
16.2 ± 0.2	BC1710		124 ± 11	
16.0 ± 0.2			81 ± 7	
14.7 ± 0.2			14.5 ± 1.3	
14.3 ± 0.2			5.1 ± 0.5	
13.4 ± 0.3			0.8 ± 0.1	
13.0 ± 0.3			0.7 ± 0.1	

*For data on other reaction products cf. [5, 6].

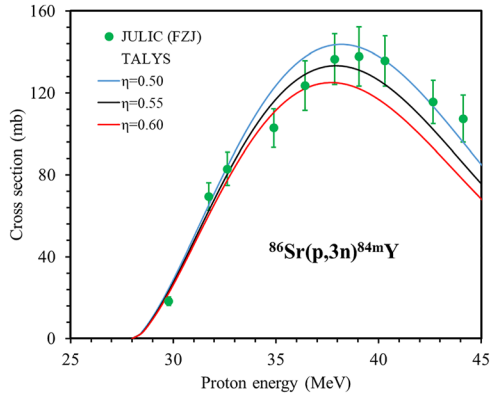


Figure 2: Excitation function for the formation of the radionuclide ^{84m}Y in proton irradiation of an enriched ^{86}Sr target. The calculated data using the TALYS code are presented for three different η values.

regard to ^{82m}Rb , our measured values and the earlier data by Levkovskii [22], which were normalised by multiplying with a factor of 0.75 [23], agree fairly well (Figure 3). The excitation function follows a smooth curve and it is reproduced by the TALYS calculation. In the case of ^{85g}Sr (Figure 4), besides our data, the normalised cross section values reported by Levkovskii [22], are also given. Our data show a very smooth trend and are reproduced by the TALYS calculation. The data by Levkovskii are 2–6 times lower compared to the data of this work. The reasons for this difference are not clear. His data might only represent the $^{86}\text{Sr}(p,pn)^{85g}\text{Sr}$ reaction cross section, not including the contribution through the decay of the precursors, or there might be other reasons. But since no details are available, it not possible to analyse them critically.

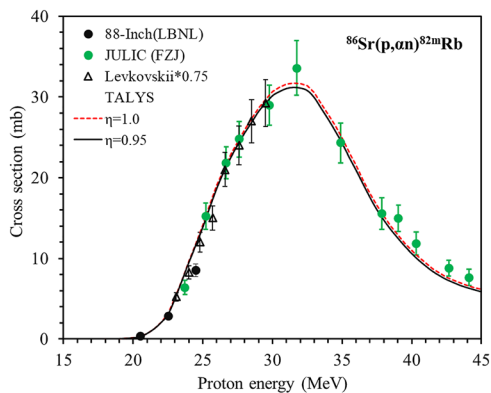


Figure 3: Excitation function for the formation of the radionuclide ^{82m}Rb in proton irradiation of an enriched ^{86}Sr target. The calculated data using the TALYS code are presented for two different η values.

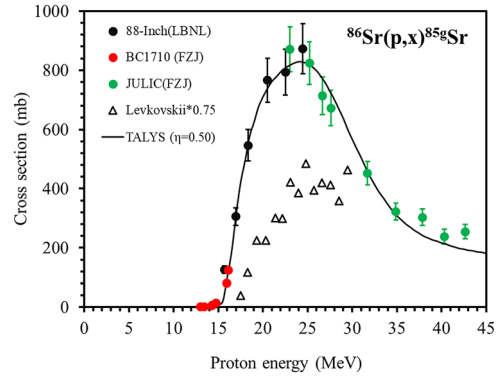


Figure 4: Excitation function for the formation of the radionuclide ^{85g}Sr in proton irradiation of an enriched ^{86}Sr target. Our experimental data and the results of the model calculation represent cumulative cross sections.

5.1.2 Calculated yields of the investigated products at accelerators

From the fitted excitation functions of the reaction products ^{86m}Y , ^{86g}Y , ^{85m}Y , ^{85g}Y , ^{83}Rb , and ^{84}Rb reported previously [5, 6] and of the products ^{84m}Y , ^{85g}Sr , and ^{82m}Rb described in this work, the integral yield A (i.e. the decay rate at EOB) of each product was calculated using the formula given below (taken from [1]):

$$A = \frac{N_L \cdot H}{M} I (1 - e^{-\lambda t}) \int_{E_1}^{E_2} \left(\frac{dE}{d(\rho x)} \right)^{-1} \sigma(E) dE \quad (1)$$

where N_L is the Avogadro number, H the enrichment of ^{86}Sr , M the mass number of the target isotope, I the proton current (particles s^{-1}), λ the decay constant of the product

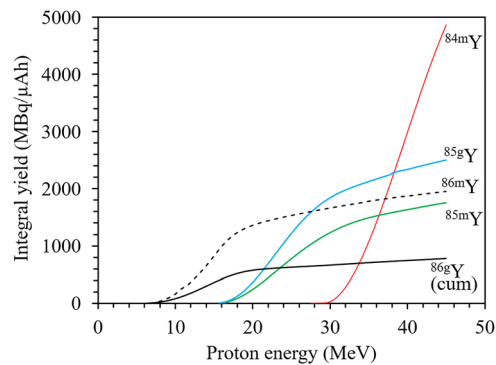


Figure 5: Integral yields of the radionuclides $^{84m,85m,85g,86m,86g}\text{Y}$ calculated from the measured excitation functions of the $^{86}\text{Sr}(p,x)$ -processes, assuming an irradiation time of 1 h at a proton beam current of $1 \mu\text{A}$. The data are shown as a function of the proton energy. The excitation function of ^{84m}Y was determined in this work; those other products were adopted from our earlier works [5, 6]. The yield for ^{86g}Y is cumulative (see text).

under consideration and t is the time of irradiation. The term $\left(\frac{dE}{d(\rho x)}\right)$ describes the stopping power, $\sigma(E)dE$ the cross section at energy E , and E_1 and E_2 are the lower and upper energy limits of the proton in the target. In each calculation, the beam current was assumed as $1 \mu\text{A}$ and the irradiation time as 1 h. The results for the Y-isotopes are shown in Figure 5. The cross sections for the formation of ^{84m}Y and ^{86m}Y are not high, but the calculated activities are rather high due to their short half-lives. The curve for the ^{86g}Y gives the cumulative decay rate, i.e. a sum of the directly formed ^{86g}Y and that formed through the complete decay of ^{86m}Y (which is very small when adjusted to the half-life of ^{86g}Y). The yields of the various individual contributing reactions to the formation of ^{85g}Sr are shown in Figure 6, and those for ^{82m}Rb , ^{83}Rb , and ^{84}Rb in Figure 7. From those yield

data the appropriate energy range for the production of a particular radionuclide via a given reaction could be deduced.

5.2 Yield of ^{85g}Sr via the $^{84}\text{Sr}(n,\gamma)$ process

The fluxes of thermal neutrons and epithermal neutrons at the irradiation position in the TRIGA Mark-II reactor, Savar [cf. 14] at the reactor power of 500 kW were determined via the $^{197}\text{Au}(n,\gamma)^{198}\text{Au}$ reaction and the results obtained amounted to $5.71 \times 10^{12} \text{ ncm}^{-2}\text{s}^{-1}$ and $3.06 \times 10^{11} \text{ ncm}^{-2}\text{s}^{-1}$, respectively. The fast neutron flux at the same irradiation position was determined using the monitor reaction $^{58}\text{Ni}(n,p)^{58}\text{Co}$ and the well characterized shape and intensity of the neutron spectrum over the energy range of 0.5–20 MeV [14]. The spectrum averaged cross section of the $^{58}\text{Ni}(n,p)^{58}\text{Co}$ reaction adopted was $91.2 \pm 5.5 \text{ mb}$. From this cross section value and the measured ^{58}Co radioactivity, the fast neutron flux above 0.5 MeV was determined as $3.95 \times 10^{12} \text{ ncm}^{-2}\text{s}^{-1}$. Under the above experimental condition, the measured activity of ^{85g}Sr was $42.7 \pm 2.6 \text{ kBq/g}$ of Sr at 20 min irradiation. For comparison, we also calculated the yield of ^{85g}Sr theoretically for a 20 min irradiation using the neutron fluxes determined in this work and adopting the cross section data reported in the literature [24–28]. The results are given in Table 3. The activity of ^{85g}Sr obtained for thermal and epithermal component is different for each calculation due to different cross sections reported by various groups [24–27]. Regarding the contribution of the fast neutrons to the formation of ^{85g}Sr , no experimental data were available. We therefore estimated the (n,γ) cross section averaged for the fast neutron spectrum of TRIGA Mark II reactor, based on the values given in the evaluated file ENDF/B-VIII.0 [28]; the integrated value obtained was 71.32 mb. By using that value, the amount of the product ^{85g}Sr formed in the irradiation by fast neutrons was estimated, and that result is also given in Table 3. This contribution amounts to about 3% of the total calculated ^{85g}Sr activity. Considering all the yield data we conclude that our experimental yield of $42.7 \pm 2.6 \text{ kBq/g}$ of Sr is close to the value of $46.5 \pm 8.3 \text{ kBq/g}$ of Sr obtained by calculation using the most recent measurement by Krane [24].

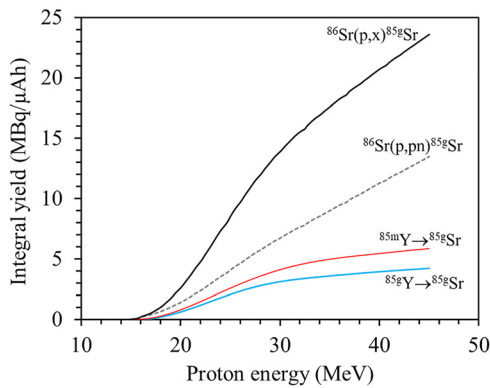


Figure 6: Integral yield of the radionuclide ^{85g}Sr calculated from the measured excitation function of the $^{86}\text{Sr}(p,x)$ -process, assuming an irradiation time of 1 h at a proton beam current of $1 \mu\text{A}$. The data are shown as a function of the proton energy. The yields of the three major contributing processes to the cumulative yield, i.e. the $^{86}\text{Sr}(p,pn)$ -reaction and the decay of the precursors ^{85m}Y and ^{85g}Y , are also shown.

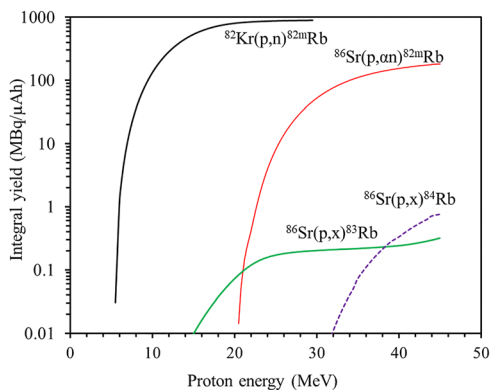


Figure 7: Integral yields of the radionuclides $^{82m,83,84}\text{Rb}$ calculated from the measured excitation functions of the $^{86}\text{Sr}(p,x)$ -processes, and the ^{82m}Rb yield also from the $^{82}\text{Kr}(p,n)$ -process [11, 12], assuming an irradiation time of 1 h at a proton beam current of $1 \mu\text{A}$. The data are shown as a function of the proton energy.

5.3 Production possibilities

Based on the calculated yields, we discuss the production possibilities of the three useful or potentially useful radionuclides mentioned in the Introduction, namely ^{85g}Sr , ^{83}Rb , and ^{82m}Rb , in no-carrier added form, using a

Table 3: Measured and calculated yields of ^{85}gSr via neutron induced reaction at TRIGA reactor.

a) Measured ^{85}gSr activity at TRIGA Mark-II reactor							
Sample	Neutron flux ($\text{ncm}^{-2}\text{s}^{-1}$)			Measured activity of ^{85}gSr (kBq/g of Sr) (^{nat}Sr target, 20 min irradiation at 500 kW)			
	Thermal	Epithermal	Fast	Total			
$^{nat}\text{SrCl}_2$	5.71×10^{12}	3.06×10^{11}	3.95×10^{12}	42.7 ± 2.6			
b) Calculated ^{85}gSr activity based on available literature cross section data and the above neutron fluxes							
Source	Thermal cross section (mb)	Resonance integral (mb)	Calculated activity of ^{85}gSr (kBq/g of Sr) (^{nat}Sr target, 20 min irradiation at 500 kW)				
			Thermal	Epithermal	Fast	Total	
Krane [24]	718	12,270	23.42	21.46	1.61	46.5 ± 8.3	
Heft [26]	822	11,310	26.82	19.78	1.61	48.2 ± 2.8	
Van der Linden et al. [27]	891	23,000	29.09	40.22	1.61	70.9 ± 9.3	
Farina Arbocco et al. [25]	700	14,500	22.84	25.36	1.61	49.8 ± 1.1	
ENDF/B-VIII.0 [28]	822	11,390	26.83	19.92	1.61	48.4	

30 MeV proton beam. There is a special focus on this energy because a new cyclotron with this energy (IBA CPx30) has been recently installed at FZJ. The calculated data via various routes for each radionuclide for a suitable energy range are given in Table 4.

5.3.1 ^{85}gSr ($T_{1/2} = 64.85$ day)

5.3.1.1 Carrier-added product

The total calculated yield of this relatively long-lived radionuclide via the $^{86}\text{Sr}(p,x)^{85}\text{gSr}$ process is rather high. For $E_p = 30 \rightarrow 16$ MeV it amounts to $14.2 \text{ MBq}/\mu\text{Ah}$. Thus, if a 96.4% enriched ^{86}Sr target is irradiated with protons in the above energy window ($0.6535 \text{ g } ^{86}\text{SrCO}_3$) with a beam current of $10 \mu\text{A}$ for 10 h, the radioactivity of ^{85}gSr would amount to 0.619 GBq , and the specific activity would be 1.609 GBq/g of Sr. Due to the very high cost of the enriched target material, however, it is unlikely that this production route would be used, particularly because the target material cannot be recycled (since the target and the

product are two isotopes of the same element). On the other hand, from the cross section data we estimate that under the above-mentioned conditions and using a $^{nat}\text{SrCO}_3$ target, ^{85}gSr could be obtained in quantities of about 71.5 MBq with a specific activity of about 185.7 MBq/g of Sr. In that case, however, a chemical separation of Sr from radioyttrium and radorubidium would be necessary. This should, however, not be a big problem. An efficient solid phase extraction chromatographic separation of the three elements from proton-irradiated $^{nat}\text{SrCO}_3$ has already been developed at FZJ [29].

As regards the production of ^{85}gSr at the TRIGA reactor, from our measured yields we estimate that a 10 h irradiation at the full reactor power of 3 MW would lead to about 7.7 MBq of $^{85}\text{gSr}/\text{g}$ of ^{nat}Sr . The yield and specific activity could be increased by using an isotopically enriched $^{84}\text{SrCl}_2$ target. But the cost of the enriched ^{84}Sr target is even higher than that of the enriched ^{86}Sr target used in cyclotron production. We therefore conclude that using a natural Sr target the production of carrier-added

Table 4: Calculated yields of the radionuclides ^{85}gSr , ^{83}Rb , and $^{82\text{m}}\text{Rb}$ in no-carrier-added form via various proton-induced reactions.

Radionuclide	Reaction	Proton energy range (MeV)	Yield ($\text{MBq}/\mu\text{Ah}$)	Reference
^{85}gSr	$^{85}\text{Rb}(p,n)$	$17 \rightarrow 10$	2.83	[8]
	$^{nat}\text{Rb}(p,xn)$	$17 \rightarrow 10$	1.77	[10, 11]
	$^{86}\text{Sr}(p,x)^{85}\text{gSr}$	$30 \rightarrow 16$	14.2^*	[This work]
	$^{86}\text{Sr}(p,2n)^{85\text{m,g}}\text{Y}$	$30 \rightarrow 16$	7.23	[This work]
	$\xrightarrow{\text{precursor}} ^{85}\text{gSr}$			
^{83}Rb	$^{83}\text{Kr}(p,n)$	$17 \rightarrow 10$	2.62	[11]
	$^{86}\text{Sr}(p,\alpha)$	$30 \rightarrow 15$	0.2	[This work]
$^{82\text{m}}\text{Rb}$	$^{82}\text{Kr}(p,n)$	$17 \rightarrow 10$	550	[11, 12]
	$^{86}\text{Sr}(p,\alpha n)$	$30 \rightarrow 20$	52	[This work]

*Carrier-added product.

^{85g}Sr would be more effective at a medium-sized cyclotron than at a medium-flux nuclear reactor. However, if a ^{84}Sr target of about 50% enrichment could be made available, or if the irradiation time could be increased to about 100 h, the yield and specific activity of ^{85g}Sr via both the production routes (reactor or cyclotron) would be comparable. Very long irradiations (4–6 months) in a nuclear reactor would improve both the quantity and specific activity of ^{85g}Sr considerably.

5.3.1.2 No-carrier-added product

Besides the production of carrier-added ^{85g}Sr at a cyclotron or in a nuclear reactor, we also analysed the $^{85m,g}\text{Y} \rightarrow ^{85g}\text{Sr}$ precursor route which leads to no-carrier-added ^{85g}Sr . From the calculated yields of $^{85m}\text{Y} \rightarrow ^{85g}\text{Sr}$ and $^{85}\text{Y} \rightarrow ^{85g}\text{Sr}$ given in Figure 6, one obtains a value of 7.23 MBq/ μAh of ^{85g}Sr over $E_p = 30 \rightarrow 16$ MeV. Thus a 10 h irradiation of a 96.4% enriched $^{86}\text{SrCO}_3$ target at about 10 μA proton beam current could lead to about 619 MBq of no-carrier-added ^{85g}Sr . In this process, however, two separation steps would be involved; first, isolation of the parents $^{85m,g}\text{Y}$ and then, after their decay, separation of the daughter ^{85g}Sr . The separation of radioyttrium from the ^{86}Sr target is easily done through adsorption on $\text{La}(\text{OH})_3$, as described earlier [cf. 30, 31]. The subsequent removal of the no-carrier-added product ^{85g}Sr from the bulk of La could then possibly be achieved via a chromatographic method. A yet another possible production route for ^{85g}Sr in no-carrier-added form involves the interaction of enriched ^{85}Rb [8] or $^{\text{nat}}\text{Rb}$ [9, 10] with protons. Those studies were performed in connection with the production of ^{82}Sr which is the parent of ^{82}Rb in a generator system (see Introduction). The radionuclide ^{85g}Sr formed therein is a disturbing impurity. But if proper energy ranges are chosen, ^{85g}Sr can possibly be produced in a pure form. From the excitation functions of those processes the calculated ^{85g}Sr yields over the respective suitable energy ranges are given in Table 4. Apparently the yield of ^{85g}Sr is the highest via the $^{85}\text{Rb}(\text{p},\text{n})$ -reaction but, as mentioned above, the indirect precursor route also appears promising. The costs of the highly enriched targets (^{85}Rb or ^{86}Sr) is not very different. The more effort involved in the precursor method could possibly be compensated by the advantage that ^{85g}Sr would be obtained as a by-product in the production of the medically important radionuclide ^{86g}Y .

5.3.2 ^{83}Rb ($T_{1/2} = 86.2$ day)

The calculated production yield of this relatively long lived radionuclide via the $^{86}\text{Sr}(\text{p},\text{x})^{83}\text{Rb}$ process over $E_p = 30 \rightarrow 15$ MeV amounts to about 0.2 MBq/ μAh . Over this energy range, it is primarily formed via the

$^{86}\text{Sr}(\text{p},\alpha)^{83}\text{Rb}$ reaction [6]. The calculated yield via the $^{83}\text{Kr}(\text{p},\text{n})^{83}\text{Rb}$ reaction [11] is about 2.6 MBq/ μAh over $E_p = 17 \rightarrow 10$ MeV. In both cases enriched target material is needed. The advantage of the method investigated in this work, however, is that gas targetry is not needed. The practically achieved production yield via both processes would be <100 MBq, but this amount may be sufficient for tracer studies.

5.3.3 ^{82m}Rb ($T_{1/2} = 6.47$ h)

The production yield of this short-lived radionuclide over $E_p = 30 \rightarrow 20$ MeV amounts to about 52 MBq/ μAh . It is primarily formed via the $^{86}\text{Sr}(\text{p},\alpha)^{82m}\text{Rb}$ reaction. The $^{82}\text{Kr}(\text{p},\text{n})^{82m}\text{Rb}$ reaction, on the other hand, leads to a yield of about 550 MBq/ μAh over $E_p = 17 \rightarrow 10$ MeV. The use of the latter reaction has been even practically demonstrated [12]. So this reaction is the method of choice. The cost of the enriched targets ^{82}Kr and ^{86}Sr are comparable. The only advantage of the $^{86}\text{Sr}(\text{p},\alpha)^{82m}\text{Rb}$ reaction could thus be that gas targetry is not required and ^{82m}Rb is obtained as a by-product of ^{86g}Y production.

6 Conclusions

New cross sections of the $^{86}\text{Sr}(\text{p},\alpha)^{82m}\text{Rb}$, $^{86}\text{Sr}(\text{p},3\text{n})^{84m}\text{Y}$, and $^{86}\text{Sr}(\text{p},\text{x})^{85g}\text{Sr}$ reactions from their respective thresholds up to 44.1 MeV were obtained through measurements on 96.4% enriched $^{86}\text{SrCO}_3$ as target. The measured values for all three radionuclides are reproduced well by the TALYS calculation. The data for ^{84m}Y formation are the first one. The discrepancies in the existing data of the excitation function of the $^{86}\text{Sr}(\text{p},\text{x})^{85g}\text{Sr}$ reaction have been removed and the database has been strengthened up to 42.7 MeV. The production route $^{\text{nat}}\text{Sr}(\text{p},\text{x})^{85g}\text{Sr}$ at a 30 MeV cyclotron could compete with the $^{\text{nat}}\text{Sr}(\text{n},\text{y})$ -route at a reactor, if the specific activity is not a problem. An alternative $^{86}\text{Sr}(\text{p},2\text{n})^{85m,g}\text{Y} \rightarrow ^{85g}\text{Sr}$ precursor route investigated in this work leads to no-carrier-added ^{85g}Sr in sufficient quantity. The $^{86}\text{Sr}(\text{p},\alpha)^{82m}\text{Rb}$ reaction could be a suitable route for small scale production of ^{82m}Rb because gas targetry is not required and ^{82m}Rb is obtained as a by-product of ^{86g}Y production.

Acknowledgments: M.S. Uddin thanks the Alexander von Humboldt (AvH) Foundation in Germany for financial support and the authorities of Bangladesh Atomic Energy Commission and Ministry of Science and Technology, Dhaka, Bangladesh, for granting leave of absence to

conduct these experiments abroad at FZJ. The LBNL component of this research was supported by the U.S. Department of Energy Isotope Program, managed by the Office of Science for Isotope R&D and Production under contract DE-AC02-05CH11231. We all thank the operation crews of the three cyclotrons (88-Inch at LBNL; BC1710 and JULIC at FZJ) and of the TRIGA reactor at AERE, Savar, for experimental assistance.

Author contributions: All the authors have accepted responsibility for the entire content of this submitted manuscript and approved submission.

Research funding: None declared.

Conflict of interest statement: The authors declare no conflicts of interest regarding this article.

References

1. Qaim S. M. *Medical Radionuclide Production—Science and Technology*; De Gruyter: Berlin/Boston, 2020; pp. 1–288.
2. Radioisotopes in Medicine; World Nuclear Association: Tower House, London, UK. world-nuclear.org/Information-Library/Non-power-nuclear-applications/Radioisotopes-Research/Radioisotopes-in-Medicine.aspx (accessed Apr, 2022).
3. Qaim S. M., Scholten B., Neumaier B. New developments in the production of theranostic pairs of radionuclides. *J. Radioanal. Nucl. Chem.* 2018, *318*, 1493–1509.
4. Rösch F., Herzog H., Qaim S. M. The beginning and development of the theranostic approach in nuclear medicine, as exemplified by the radionuclide pair ^{86}Y and ^{90}Y . *Pharmaceuticals* 2017, *10*, 56.
5. Uddin M. S., Scholten B., Basunia M. S., Sudár S., Spellerberg S., Voyles A. S., Morrell J. T., Zaneb H., Rios J. A., Spahn I., Bernstein L. A., Qaim S. M., Neumaier B. Accurate determination of production data of the non-standard positron emitter ^{86}Y via the $^{86}\text{Sr}(p,n)$ -reaction. *Radiochim. Acta* 2020, *108*, 747–756.
6. Uddin M. S., Basunia M. S., Sudár S., Scholten B., Spellerberg S., Voyles A. S., Morrell J. T., Fox M. B., Spahn I., Felden O., Gebel R., Bernstein L. A., Neumaier B., Qaim S. M. Excitation functions of proton-induced nuclear reactions on ^{86}Sr , with particular emphasis on the formation of isomeric states in ^{86}Y and ^{85}Y . *Eur. Phys. J. A* 2022, *58*, 67.
7. NuDat 3.0. <https://www.nndc.bnl.gov/nudat3/>.
8. Kastleiner S., Qaim S. M., Nortier F. M., Blessing G., van der Walt T. N., Coenen H. H. Excitation functions of $^{85}\text{Rb}(p,xn)^{85m,g,83,82,81}\text{Sr}$ reactions up to 100 MeV: integral tests of cross sections data, comparison of production routes of ^{83}Sr and thick target yield of ^{82}Sr . *Appl. Radiat. Isot.* 2002, *56*, 685–695.
9. Ido T., Hermanne A., Ditrői F., Szűcs Z., Mahunka I., Tárkányi F. Excitation functions of proton induced nuclear reactions on ^{nat}Rb from 30 to 70 MeV. Implication for the production of ^{82}Sr and other medically important Rb and Sr radioisotopes. *Nucl. Instrum. Methods Phys. Res. Sect. B* 2002, *194*, 369–388.
10. Qaim S. M., Steyn G. F., Spahn I., Spellerberg S., van der Walt T. N., Coenen H. H. Yield and purity of ^{82}Sr produced via the $^{nat}\text{Rb}(p,xn)^{82}\text{Sr}$ process. *Appl. Radiat. Isot.* 2007, *65*, 247–252.
11. Kovács Z., Tárkányi F., Qaim S. M., Stöcklin G. Excitation functions for the formation of some radioisotopes of rubidium in proton induced nuclear reactions on ^{nat}Kr , ^{82}Kr and ^{83}Kr with special reference to the production of ^{81}Rb (^{61m}Kr) generator radionuclide. *Appl. Radiat. Isot.* 1991, *42*, 329–335.
12. Kovács Z., Tárkányi F., Qaim S. M., Stöcklin G. Production of 6.5 h ^{82m}Rb via the $^{82}\text{Kr}(p,n)$ -process at a low-energy cyclotron—a potential substitute for ^{82}Rb . *Appl. Radiat. Isot.* 1991, *42*, 831–834.
13. Hermanne A., Ignatyuk A. V., Capote R., Carlson B. V., Engle J. W., Kellett M. A., Kibedi T., Kim G., Kondev F. G., Hussain M., Lebeda O., Luca A., Nagai Y., Naik H., Nichols A. L., Nortier F. M., Suryanarayana S. V., Takács S., Tárkányi F., Verpelli M. Reference cross sections for charged-particle monitor reactions. *Nucl. Data Sheets* 2018, *148*, 338–382.
14. Uddin M. S., Sudár S., Hossain S. M., Khan R., Zulquarnain M. A., Qaim S. M. Fast neutron spectrum unfolding of a TRIGA Mark II reactor and measurement of spectrum-averaged cross sections: integral tests of differential cross sections of neutron threshold reactions. *Radiochim. Acta* 2013, *101*, 613–620.
15. Fitzgerald J. *JF Computing Services, 17 Chapel Road, Stanford in the Vale, Oxfordshire, SN7 8LE*. Copyright © Jim Fitzgerald 1991–2016 (accessed Oct 8, 2016).
16. Uddin M. S., Qaim S. M., Scholten B., Basunia M. S., Bernstein L. A., Spahn I., Neumaier B. Positron emission intensity in the decay of ^{86g}Y for use in dosimetry studies. *Molecules* 2022, *27*, 768.
17. Calamand A. Cross sections for fission neutron spectrum induced reactions. In *Handbook on Nuclear Activation Cross Sections*. Technical Report No. 156, IAEA: Vienna, 1974; pp. 273.
18. Koning A. J., Hilaire S., Duijvestijn M. C. TALYS-1.0. In *Proc. International Conference on Nuclear Data for Science and Technology, April 22–27, 2007*; Bersillon O., Günsing F., Bauge E., Jacquemin R., Leray S., Eds. EDP Sciences: Nice, France, 2008; pp. 211–214.
19. Koning A. J., Rochman D., van der Marck S. C., Kopecky J., Sublet J. Ch., Pomp S., Sjostrand H., Forrest R., Bauge E., Henriksson H., Cabellos O., Goriely S., Leppanen I., Leeb H., Plompen A., Mills R. *TENDL-2019: TALYS-Based Evaluated Nuclear Data Library*; IAEA: Vienna, 2019.
20. Capote R., Herman M., Obložinsky P., Young P., Goriely S., Belgia T., Ignatyuk A., Koning A. J., Hilaire S., Plujko V., Avrigeanu M., Chadwick O. B. M., Fukahori T., Kailas S., Kopecky J., Maslov V., Reffo G., Sin M., Soukhovitskii E., Talou P., Yinlu H., Zhigang G. RIPL 3: reference input parameter library for calculation of nuclear reactions and nuclear data evaluations. *Nucl. Data Sheets* 2009, *110*, 3107.
21. Sudár S., Qaim S. M. Mass number and excitation energy dependence of the $\Theta_{\text{eff}}/\Theta_{\text{rig}}$ parameter of the spin cut-off factor in the formation of an isomeric pair. *Nucl. Phys.* 2018, *979*, 113–142.
22. Levkovskii V. N. Activation cross sections for nuclides of average masses ($A=40-100$) by protons and alpha-particles with average energies ($E=10-50$ MeV). In *Experiment and Systematics*; Inter-Vesy: Moscow, 1992.
23. Qaim S. M., Sudár S., Scholten B., Koning A. J., Coenen H. H. Evaluation of excitation functions of $^{100}\text{Mo}(p,d+pn)^{99}\text{Mo}$ and $^{100}\text{Mo}(p,2n)^{99m}\text{Tc}$ reactions: estimation of long-lived Tc-impurity and its implication on the specific activity of cyclotron-produced ^{99m}Tc . *Appl. Radiat. Isot.* 2014, *85*, 101–113.

24. Krane K. S. Cross sections and isomer ratios in the $\text{Rb}(n,\gamma)$ and $\text{Sr}(n,\gamma)$ reactions. *Eur. Phys. J. A* 2021, 57, 19.
25. Farina Arbocco F., Vermaercke P., Smits K., Sneyers L., Strijckmans K. Experimental determination of k_0 , Q_0 factors, effective resonance energies and neutron cross-sections for 37 isotopes of interest in NAA. *J. Radioanal. Nucl. Chem.* 2014, 302, 655.
26. Heft R. E. A consistent set of nuclear-parameter values for absolute instrumental neutron activation analysis. In *Conf. on Computers in Activation Analysis and Gamma-ray Spectroscopy*; Department of Energy: Washington, DC, 1978; pp. 495–510.
27. Van der Linden R., De Corte F., Van Den Winkel P., Hoste J. A compilation of infinite dilution resonance integrals. *J. Radioanal. Chem.* 1972, 11, 133.
28. ENDF/B-VIII.0, 2018; National Nuclear Data Center, Brookhaven National Laboratory: USA. Database version of 20 December 2018. <https://www.nndc.bnl.gov/ndf/>.
29. Breunig K. *Radiochemische untersuchungen zur abtrennung von trägerarmem radioyttrium aus bestrahlten strontiumtargets mittels festphasenextraktion*. M.Sc. thesis, Köln University, FZJ, 2011.
30. Rösch F., Qaim S. M., Stöcklin G. Production of the positron emitting radioisotope ^{86}Y for nuclear medical application. *Appl. Radiat. Isot.* 1993, 44, 677–681.
31. Ketterer K., Linse K.-H., Spellerberg S., Coenen H. H., Qaim S. M. Radiochemical studies relevant to the production of ^{86}Y and ^{88}Y at a small-sized cyclotron. *Radiochim. Acta* 2002, 90, 845–849.